UDK 669.1.017:620.193
Original scientific article/Izvirni znanstveni članek

ISSN 1580-2949
Mater. Tehnol.

EFFECT OF CORROSION ON THE DYNAMIC BEHAVIOUR OF AISI 4140, AISI 4340, AND AISI 5140 STEELS EXPOSED TO 3.5 *w*/% NaCl ENVIRONMENT

VPLIV KOROZIJE NA DINAMIČNO OBNAŠANJE JEKEL VRST AISI 4140, AISI 4340, IN AISI 5140, IZPOSTAVLJENIH VODNI RAZTOPINI S 3,5 *w*/% NaCl

Mesut Yıldız*, Hüsnü Gerengi

Düzce University, Faculty of Engineering, Department of Mechanical Engineering, Düzce, Turkey

Prejem rokopisa – received: 2024-05-22; sprejem za objavo – accepted for publication: 2024-09-11

doi:10.17222/mit.2024.1199

Material loss due to corrosion can weaken the structural integrity of systems and potentially lead to failure if timely action is not taken. Such deterioration adversely affects the dynamic behavior of metals. This study deals with the post-corrosion changes in the dynamic behavior of AISI 4140, AISI 4340 and AISI 5140 metals after exposure to 3.5 *w*/% NaCl for 1, 7, 15 and 30 days. Electrochemical impedance spectroscopy (EIS) and dynamic electrochemical impedance spectroscopy (dynamic EIS) were used to elucidate the corrosion mechanisms. Modal analysis and finite element method (FEM) were used to characterize dynamic behavior changes. In addition, scanning electron microscopy (SEM-EDS) was used to analyze changes in the surface morphology after corrosion. The results showed a decrease in the corrosion resistance of AISI 4140, AISI 4340 and AISI 5140 metals over time, although there was an improvement after 30 days. The electrochemical test results indicated that the metal with the highest corrosion resistance in the 3.5 *w*/% NaCl environment was AISI 4340, while AISI 5140 showed the lowest resistance. In particular, natural frequency values showed a decreasing trend with increasing corrosion exposure time, accompanied by discernible changes in mode shapes.

Keywords: corrosion, dynamic behavior, steel

Izgube materiala zaradi korozije lahko oslabijo strukturno integriteto sistema in potencialno vodijo do odpovedi, če ne ukrepamo pravočasno. Takšne korozijske poškodbe lahko še posebej močno vplivajo na dinamično obremenjene sisteme oziroma materiale. V tem članku avtorji opisujejo študijo, ki obravnava obnašanje izbranih jekel (AISI 4140, AISI 4340 in AISI 5140) po koroziji v slanici (vodni raztopini s 3,5 *w*/% NaCl) in dinamičnem obremenjevanju. Vzorci izbranih jekel so bili v slanici različno dolgo (1, 7, 15 in 30) dni. Nato so avtorji izvedli elektro-kemijsko impedančno spektroskopijo (EIS) in dinamično elektro-kemijsko impedančno spektroskopijo (angl.: Dynamic-EIS) zato, da so pojasnili korozijske mehanizme. Za karakterizacijo sprememb dinamičnega obnašanja materialov so uporabili modalno analizo in metodo končnih elementov (FEM; angl.: finite elements method). Dodatno so uporabili še vrstično elektronsko mikroskopijo in elektronsko disperzijsko spektroskopijo (SEM-EDS) za analizo morfoloških in mikro-kemijskih sprememb površine zaradi korozije. Rezultati analiz so pokazali zmanjševanje odpornosti vzorcev iz izbranih jekel AISI 4140, AISI 4340 in AISI 5140 s podaljševanjem njihovega zadrževanja v slanici. Elektro-kemijski testi so pokazali, da ima najboljšo odpornost proti koroziji jeklo AISI 4340, ki je bilo izpostavljeno vodni raztopini s 3,5 *w*/% NaCl medtem, ko je imelo najslabšo odpornost proti koroziji jeklo AISI 5140. Še posebej so bile očitne spremembe oblik in trend padanja vrednosti naravnih frekvenc s podaljševanjem časa zadrževanja vzorcev izbranih jekel v slanici.

Ključne besede: korozija, dinamično obnašanje in lastnosti jekel

1 INTRODUCTION

Mechanical systems consisting of various mechanical components such as shafts, rolling bearings and discs operate under many heavy conditions, such as overload and high speed. The most important feature expected from these systems is that they operate smoothly under these working conditions. In the case of metallic materials used in rotating systems, corrosion caused by environmental conditions can lead to material loss on the shaft surface, which can reduce the shaft's strength and affect its dynamic behavior.[1,2] For this reason, it is of great importance to determine the dynamic behavior of shafts operating at high speeds and to monitor potential problems that may emerge. Various parameters characterizing the dynamic behavior of a system are used to investigate the working conditions and performance of high-speed machines. Vibration measurements are an effective method for describing the dynamic properties of rotating machine systems, detecting manufacturing faults, malfunctions, and mechanical problems.[3] Vibration measurements are an essential tool for monitoring the health of rotating machinery and equipment. By measuring the vibration of a machine, potential problems can be identified before they lead to costly downtime or equipment failures. Therefore, the importance of vibration damping capacity as an engineering property of materials has been widely researched in recent years.[4–6] Corrosion, which occurs due to the interactions between materials and the surrounding environment, prevents the materials from

*Corresponding author's e-mail:
mesutyildiz@duzce.edu.tr (Mesut Yildiz)

performing their function, causes the metal to lose its original shape and size, reduces the performance of the material, and causes a shift in the natural frequency of the material.[7,8] Corrosion of shafts can be classified into two types: uniform corrosion, where the surface is corroded evenly, and localized corrosion, which occurs in a certain area of the surface.[9] Aryayi et al. investigated the change in the natural frequency of shafts as a result of pitting corrosion on clamped-free shafts with the finite element method. As a result of the study, it was determined that the natural frequencies of the corroded shafts decreased.[10] Li and Akid investigated the corrosion fatigue behavior of a shaft examined in air and NaCl solution. The findings indicate that pitting corrosion, which is more common in the aggressive NaCl environment, led to a reduced fatigue life of the shaft compared to the one tested in air.[11] The failure of the rear axle shaft of a three-wheeled vehicle was investigated by Singh et al. The analysis results confirmed that it was due to the presence of corrosion products detected on the surface of the AISI 4140 shaft that caused it to fail.[12] Zhang et al. studied the relationship between the corrosion depth and natural frequency of reinforced concrete test beams.[13] Gillich et al. developed two mathematical relations to determine the natural frequency changes caused by corrosion in metallic structures.[7]

As a result of corrosion, the natural frequencies of metals in machine systems are altered, resulting in vibratory wear failures.[10,14,15] When the operating frequency of a system is in close proximity to the natural frequency of the material, the highest degree of vibration occurs, resulting in resonance. The operation of a system with resonance results in the overlapping of energy waves, which in turn causes fractures and accidents. For that reason, the impact of corrosion on metals' natural frequencies should be quantified and the likelihood of unfavorable outcomes should be minimized without compromising the functionality of the operating system. In this study, the corrosion behaviors of AISI 4140, AISI 4340 and AISI 5140 steels exposed to a 3.5 *w*/% NaCl environment for (1, 7, 15 and 30) days were investigated with electrochemical methods, and post-corrosion natural frequency changes were determined with the modal analysis and finite element method (FEM). Although there are studies on the corrosion behavior of AISI 4140, AISI 4340 and AISI 5140 metals in a 3.5 *w*/% NaCl environment in the literature,[16–21] there is no comparable investigation, in which time-dependent experimental studies are performed. This study will contribute to the literature on the changes in corrosion resistance, natural frequencies, and vibration damping rates of AISI 4140, AISI 4340 and AISI 5140 steels over time.

2 EXPERIMENTAL PART

2.1 Materials

The chemical composition of specimens AISI 4140, AISI 4340 and AISI 5140 procured from Almina Iron-Steel Co., Turkey, are listed in **Table 1**. The samples, used as working electrodes in the electrochemical corrosion investigation, were cut into a circular shape of 25 mm in diameter and 10 mm in thickness. The working surfaces of the specimens were mechanically abraded using SiC paper ranging from 600 grit to 2000 grit. They were washed with distilled water, subsequently degreased with alcohol and dried with air before electrochemical measurements. The corrosive medium was an aqueous 3.5 *w*/% NaCl environment.

Table 1: Chemical compositions of AISI 4140, AISI 4340 and AISI 5140 steels

AISI Alloy	C	Si	Mn	P	S	Cr	Mo	Ni	Fe
4140	0.451	0.317	0.771	0.012	0.010	0.941	0.169	0.082	Bal.
4340	0.380	0.304	0.567	0.012	0.011	1.832	0.199	1.578	Bal.
5140	0.451	0.301	0.757	0.014	0.006	1.020	0.031	0.088	Bal.

2.2. Corrosion measurements

2.2.1 EIS and dynamic EIS

The corrosion resistance of the samples was tested using EIS on Gamry Reference 600 potentiostat/galvanostat/ZRA workstation in a three-electrode cell, which was composed of a reference electrode of Ag/AgCl, Pt mesh as the counter electrode and working electrodes of AISI 4140, AISI 4340 and AISI 5140 steels with exposed surface areas of 0.502 cm^2. Electrochemical tests were carried out by connecting the working electrode immersed in the test solution to the corrosion cell and stabilizing the OCP (open circuit potential) for 2 h to obtain a steady state. EIS measurements were conducted in a frequency range of 10 mHz to 100 kHz, with a 10 mV peak-to-peak amplitude signal.[22]

The dynamic EIS method that provides instant monitoring of the corrosion process on the working electrode is a better technique for corrosion measurements. Dynamic EIS was performed using a National Instruments PCI-4461 digital-to-analog card for the generation of a multi-sinusoidal current-perturbation signal. This card was also used for measuring current-perturbation and voltage-response signals. The sampling frequency was 12.8 kHz and the perturbation signal was in a frequency range of 4.5 kHz to 300 mHz.[23]

2.3. Surface analysis

Scanning electron microscopy (SEM), a surface analysis technique, was used for investigating the damage on the specimens' surfaces exposed to the corrosive medium for different periods of time. A Quanta FEG 250 (FEI,

Holland) model device equipped with an energy dispersive X-ray spectroscopy detector was used for SEM.

2.4. Modal analysis

Natural frequencies and damping ratios of materials are determined with the modal analysis, measured with an impact hammer and accelerometer.[24] The dynamic behavior of cylindrical metals under a free-free condition with a diameter of 23.5 mm and a length of 200 mm (AISI 4140, AISI 4340 and AISI 5140) before corrosion and after exposure to the 3.5 *w*/% NaCl environment for (1, 7, 15 and 30) days was examined using the modal analysis. A DYTRAN 5800B3 model force hammer with a head weight of 100 g was used to apply impact stimulation to the experimental samples. A KS78C100 model accelerometer was mounted to record the input acceleration using a KRYPTON 8xACC data acquisition device (DAQ) with a sampling rate of 20 kS/s. The natural frequencies and damping ratios obtained as a result of the modal analysis were determined using DewesoftX software.

2.5. Finite element method (FEM)

A numerical analysis of the dynamic behavior of corroded circular steels was simulated using FEM in ANSYS. The steels were considered to have a Poisson's ratio of 0.29, Young's modulus of 200 GPa and density of 7850 kg/m^3. In this study, the modal analysis results based on the FEM method were not affected by the Young's modulus. In addition, the modal analyses with FEM were calculated by reducing the thickness of the uniform corrosion layer formed on the surfaces of the metals, with the diameters of the metals measured by SEM, as shown in **Table 2**.

Table 2: Diameters of the metals before and after exposure to the corrosive medium (in mm)

Time/Metals	AISI 4140	AISI 4340	AISI 5140
Ref	23.500	23.500	23.500
After 1 day	23.496	23.498	23.497
After 7 days	23.495	23.497	23.496
After 15 days	23.495	23.495	23.496
After 30 days	23.494	23.494	23.495

3 RESULTS

3.1. Electrochemical impedance spectroscopy (EIS)

Figure 1 displays the electrochemical behavior of three steel samples after (1, 7, 15, and 30) days of exposure to 3.5 *w*/% NaCl. Nyquist diagrams of all the metals studied show an imperfect capacitive loop. According to

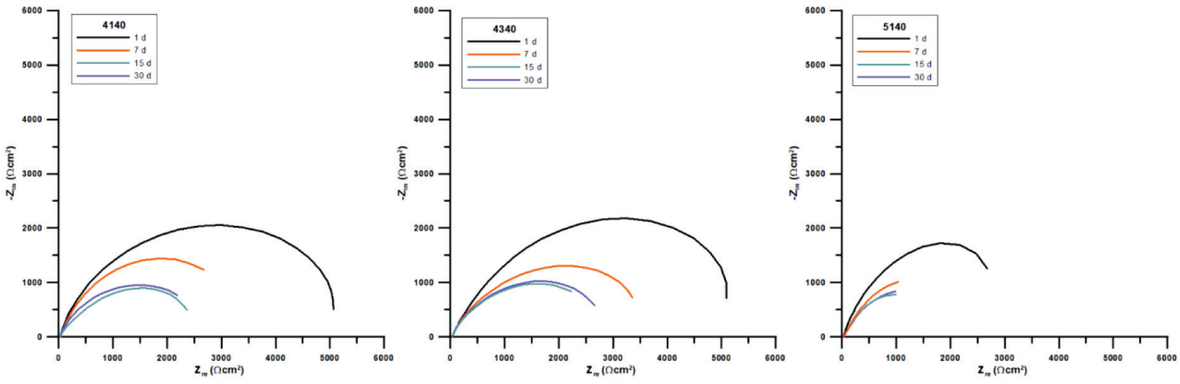

Figure 1: Nyquist diagrams for AISI 4140, AISI 4340 and AISI 5140 steels in 3.5 *w*/% NaCl

Table 3: EIS test data for AISI 4140, AISI 4340 and AISI 5140 steels in 3.5 *w*/% NaCl

Metal	Day(s)	R_s (Ω cm^2)	Q_f (μΩs^n m^{-2})	R_f (Ω cm^2)	Q_{ct} (μΩs^n m^{-2})	R_{ct} (Ω cm^2)	R_{total} (Ω cm^2)	χ^2
AISI 4140	1	32	380	1353	175	4088	5441	8.399e-05
	7	33	451	222	213	3656	3878	5.104e-05
	15	33	1374	503	662	2283	2786	1.251e-04
	30	35	889	797	637	2319	3116	1.146e-05
AISI 4340	1	33	345	1883	151	4154	6037	2.374e-04
	7	34	447	680	420	3751	4431	7.364e-05
	15	34	569	535	519	2606	3141	6.093e-05
	30	35	471	549	489	2629	3178	2.430e-05
AISI 5140	1	33	1572	1156	961	3318	4474	1.399e-04
	7	34	3028	762	1868	2624	3386	1.852e-05
	15	35	3830	222	2620	2065	2287	4.757e-05
	30	36	3147	260	2513	2195	2455	6.008e-06

the literature, this imperfection is due to the roughness or heterogeneity of the electrode surface.[25,26] **Figure 1** shows that the semicircle of AISI 4340 steel is larger than that of other metals, and the smallest semicircles belong to AISI 5140 steel. For all the steel types examined, the capacitive radii decreased up to 15 d and increased after 30 d. This suggests that there is a time-dependent behavior of the capacitive radii of steel. A possible reason for his observation could be the formation of a protective oxide layer on the surfaces of steels. Further, as the metals exposed to the environment may develop a corrosion film on their surface over time,[27] the obtained data were analyzed with ZsimpWin 3.21 software using the *R(Q(R(QR)))* equivalent circuit, where R_s is the solution resistance, R_f is the corrosion product film resistance, Q_f is the capacitance of the film, Q_{ct} is the double-layer capacitance and R_{ct} is the charge-transfer resistance. The results are listed in **Table 3**.

The $\chi 2$ values in **Table 3** demonstrate that the applied equivalent circuit model is appropriate. It is clearly seen that the highest R_f, R_{ct} and R_t values were obtained for AISI 4340 steel while the lowest ones were obtained for AISI 5140 steel. In addition, while resistance values decreased for the first 15 d, Q_f and Q_{dl} values increased. Moreover, after 30 d, the R values increased and Q values decreased for all three samples. The corrosion resistance of AISI 4340 metal is higher due to its higher ratio of Cr and Ni in its chemical composition compared to the other two metals. Alloying elements Cr and Ni form a protective oxide layer on the surface of the metal, which acts as a barrier against corrosive agents.[28,29] This oxide layer helps to prevent the penetration of moisture

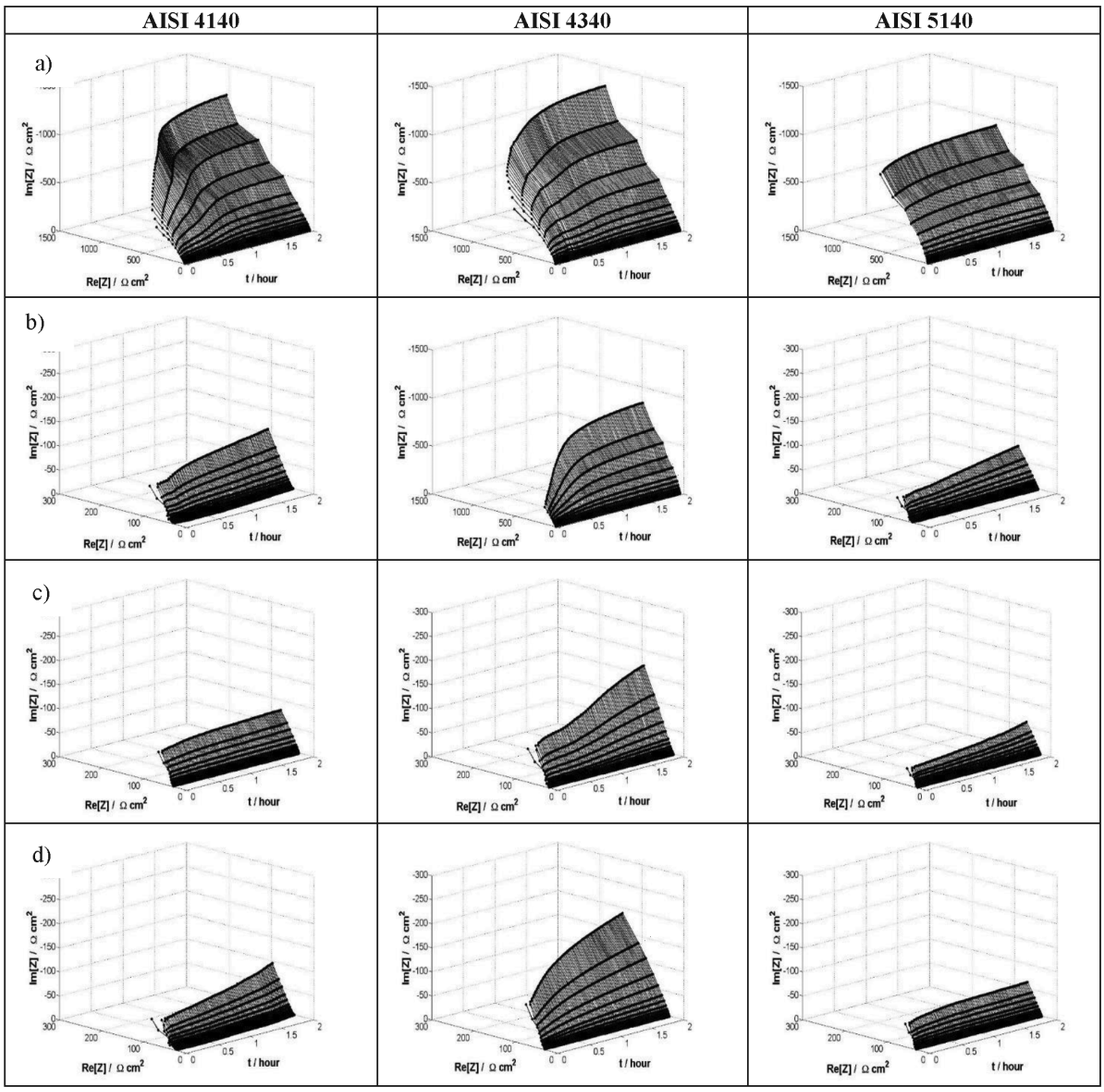

Figure 2: Dynamic-EIS plots of AISI 4140, AISI 4340, and AISI 5140 steels obtained in 3.5 *w*/% NaCl environment: a) 1 d, b) 7 d, c) 15 d, d) 30 d

Table 4: Dynamic-EIS data of AISI 4140, AISI 4340 and AISI 5140 steels in 3.5 *w*/% NaCl

Metal	Day(s)	R_s (Ω cm^2)	Q ($\mu\Omega s^n$ m^{-2})	R_f (Ω cm^2)	Q ($\mu\Omega s^n$ m^{-2})	R_{ct} (Ω cm^2)	R_{total} (Ω cm^2)	χ^2
4140	1	32	362	1154	210	4033	5187	2.735e-04
	7	34	492	412	343	3091	3503	5.528e-06
	15	35	682	258	458	2283	2541	1.894e-05
	30	37	516	471	399	2331	2802	3.245e-04
4340	1	32	226	1722	189	4038	5760	3.315e-04
	7	34	356	692	305	3317	4009	5.760e-05
	15	34	573	502	456	2754	3256	3.844e-04
	30	35	484	518	353	2876	3394	2.443e-04
5140	1	32	1126	1038	1087	3174	4212	2.249e-06
	7	33	1679	361	1401	2885	3246	4.573e-04
	15	34	2236	291	1712	1987	2278	3.776e-06
	30	35	2129	307	1692	2070	2377	4.498e-06

and other corrosive substances, thereby reducing the corrosion rate. An addition of a small amount of molybdenum (less than 0.5 %) was reported to prevent corrosion in steels.[28] Furthermore, the chemical composition of AISI 4140 steel differs from that of AISI 5140 steel due to the presence of molybdenum. Therefore, the increased corrosion resistance of AISI 4140 steel compared to AISI 5140 steel can be attributed to its higher molybdenum content.

3.2. Dynamic electrochemical impedance spectroscopy (dynamic EIS)

Dynamic EIS has gained popularity in corrosion studies as a viable alternative to EIS.[30] One of the key advantages of dynamic EIS is its ability to simultaneously excite a system with all perturbation frequencies. This simultaneous excitation allows for a more comprehensive analysis of the corrosion process, providing valuable insights into the electrochemical behavior of the system under investigation. The corrosion of steels in the 3.5 *w*/% NaCl environment was studied using this method for (1, 7, 15 and 30) days. Results of dynamic EIS of AISI 4140, AISI 4340 and AISI 5140 steels obtained from the experiments in the 3.5 *w*/% NaCl environment are displayed in **Figure 2**. Dynamic EIS results were analyzed with the same software as used for the EIS results (**Figure 1**) and its parameters are presented in **Table 4**. According to the dynamic-EIS data, the impedance semicircles of all steels were largest at the end of the first day and gradually decreased to their smallest size by the 15th day. However, the graphs show that the size of the semicircles increased at the end of the 30th day. This phenomenon can be attributed to the formation of a protective oxide layer on the surface of steel, as mentioned in the EIS section.

Table 4 shows that the applied equivalent circuit model is suitable for analyzing the dynamic-EIS data, as indicated by the $\chi 2$ values. The results of the dynamic-EIS experiments yielded parameters comparable to those obtained through the EIS method. This indicates that both techniques provide consistent and reliable data. The AISI 4340 steel has the highest R_{total} values of 5760, 4009, 3256, and 3394 Ω cm^2 for (1, 7, 15, and 30) days, respectively. On the other hand, the AISI 5140 steel has the lowest R_{total} values of 4212, 3246, 2278, and 2377 Ω cm^2 for (1, 7, 15, and 30) days, respectively. The variation in the R_{total} values among the examined steels can be attributed to the presence of different alloying elements.[28,29]

3.3 Surface analysis

SEM images (1000× magnification) of metals AISI 4140, AISI 4340 and AISI 5140 after exposure to 3.5% NaCl for 1, 7, 15 and 30 days are shown in Figure 3. Corrosion products began forming on the surfaces of the metals from day one. Different oxide types that may form on a steel surface are: haematite (α-Fe_2O_3), magnetite (Fe_3O_4), maghemite (γ-Fe_2O_3), goethite (α-FeOOH), lepidocrocite (γ-FeOOH), akaganeite (β-FeOOH), feroxyhite (δ-FeOOH), iron hydroxide [$Fe(OH)_2$], and iron trihydroxide [$Fe(OH)_3$].[31] SEM images show that the surfaces of the metals corrode, resulting in the formation of goethite and lepidocrocite morphologies. These morphologies are indicative of the corrosion products that have developed over time. During the corrosion process, the oxide layers on the metal surfaces became more distinct and cracks occurred due to the breakage of the layers. During corrosion in the 3.5 *w*/% NaCl environment, iron oxide and hydroxide are formed on the surface of steel, as illustrated by the following equations (1 and 2):[32]

$$Fe + (1/2)O_2 + H_2O \rightarrow Fe(OH)_2 \quad (1)$$

$$3Fe(OH)_2 + (1/2)O_2 \rightarrow Fe_3O_4 + 3H_2O \quad (2)$$

In SEM images, a detailed examination of the metal surfaces reveals intriguing morphologies. The presence of globular structures suggests the existence of a goethite structure. These globular morphologies could be indicative of the presence of goethite, a common iron hydroxide. Additionally, flower-petal and spider-web morphol-

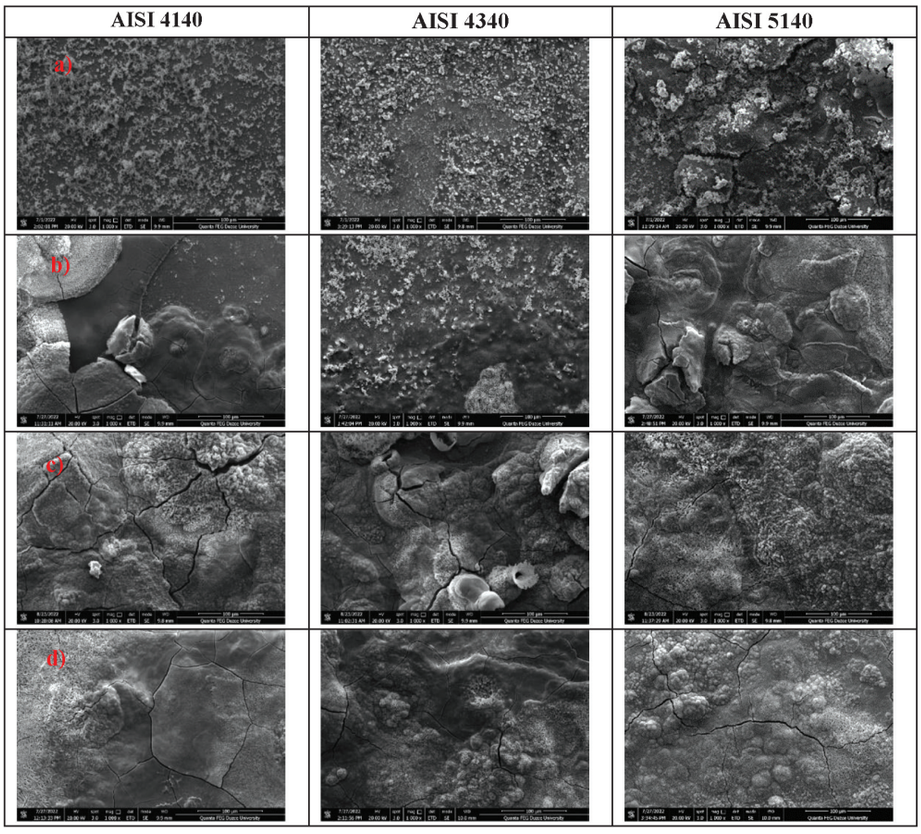

Figure 3: SEM images of AISI 4140, AISI 4340 and AISI 5140 metals after corrosion in 3.5 *w*/% NaCl environment: a) 1 d, b) 7 d, c) 15 d, d) 30 d

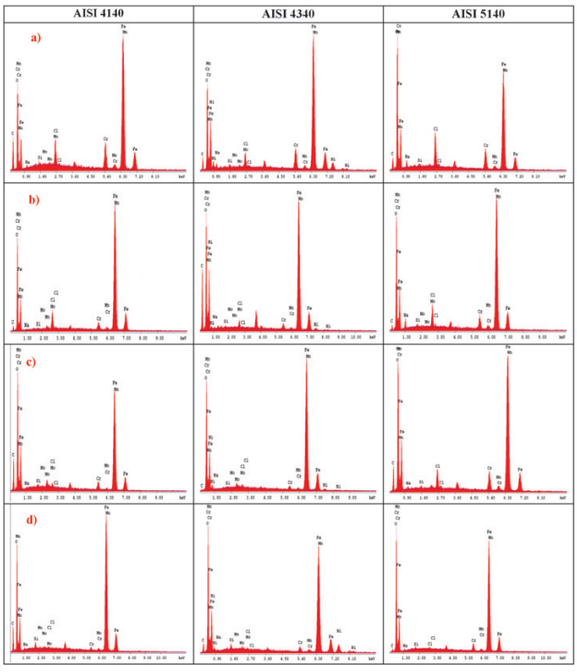

Figure 4: EDS images of AISI 4140, AISI 4340 and AISI 5140 metals after corrosion in 3.5 *w*/% NaCl environment: a) 1 d, b) 7 d, c) 15 d, d) 30 d

ogies observed on the surfaces suggest the presence of lepidocrocite.[33] Lepidocrocite is another iron hydroxide that often exhibits intricate and delicate patterns resembling flower petals or spider webs when viewed under high magnification. When steels are exposed to a Cl environment, a lepidocrocite formation is observed as the primary corrosion product on the metal surface. As the exposure time increases, a goethite structure is formed due to the deposition of Cl ions on the lepidocrocite structure.[34] The goethite structure is a more stable and protective form of corrosion compared to lepidocrocite.

The SEM-EDS images in **Figure 4** illustrate the cross-section morphologies of AISI 4140, AISI 4340, and AISI 5140 steel specimens after exposure to the 3.5 % NaCl medium for (1, 7, 15, and 30) days. The cross-section morphologies show that the corrosion layer becomes more compact and thicker as the exposure time to the environment increases for all three metals. An analysis of the EDS spectra shows that the corrosion layer on the metal surface contains the highest amount of Cl after 1 day of exposure. As the exposure time increases, the Cl content decreases and reaches its lowest level after 30 days. As mentioned above, the decrease in Cl is a result of the structural change in the corrosion layer.

3.4 Modal analysis and FEM

Table 5 presents the changes in the natural frequency and modal damping ratios of the first two mode shapes resulting from the time-dependent corrosion of AISI 4140, AISI 4340, and AISI 5140 steels in the 3.5 *w*/% NaCl environment, as obtained with the FEM and modal analysis. From the examination of the changes in natural frequencies, it is evident that the frequency values for the three metals, obtained with the FEM and modal analysis, decrease due to corrosion. This decrease in the frequency values indicates that the effect of corrosion on the stiffness of metals is greater than on the mass loss. Corrosion typically results in material deterioration and structural changes, leading to a reduction in stiffness and, consequently, a decrease in the natural frequencies of materials. Modal damping ratios, which represent the damping property of materials, are related to the dissipation or loss of energy within the system.

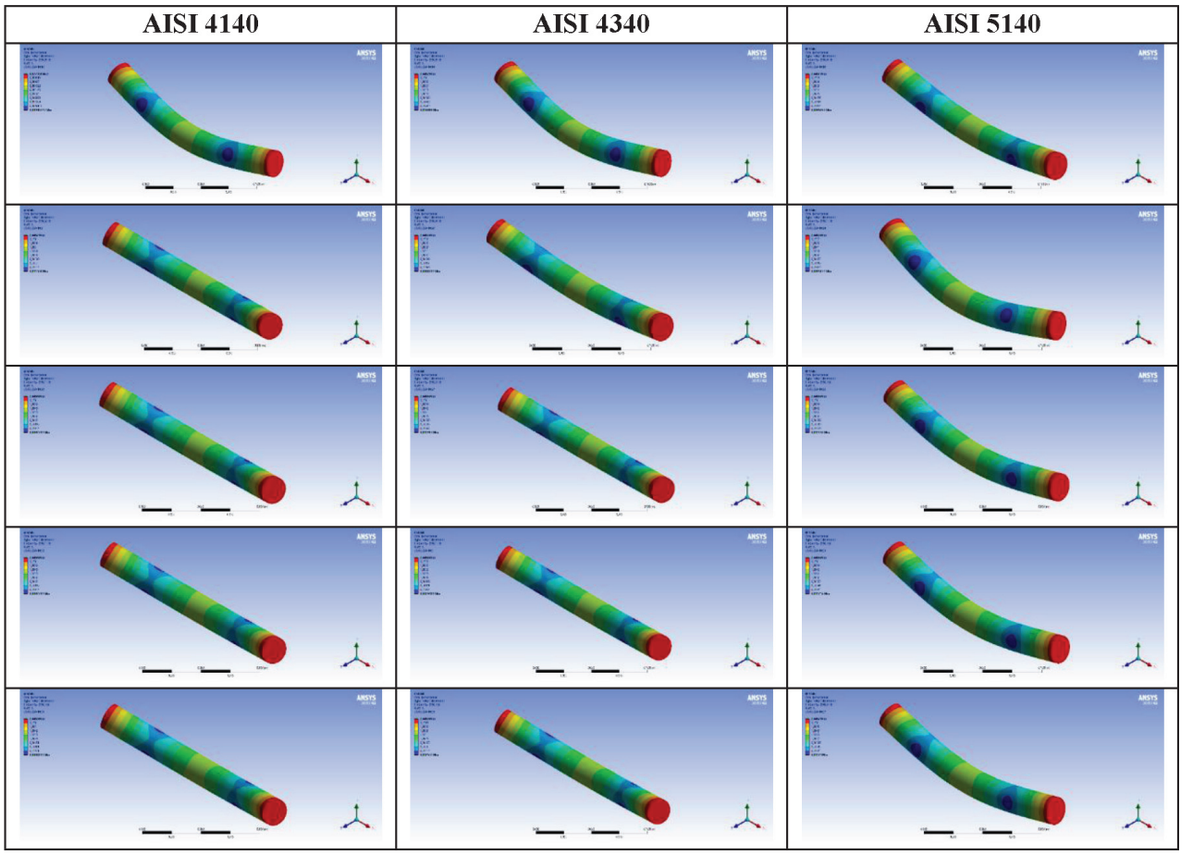

Figure 5: First natural bending mode shapes of AISI 4140, AISI 4340 and AISI 5140 steels: a) before corrosion, b) 1 d, c) 7 d, d) 15 d, e) 30 d

Table 5: Natural frequency and modal damping ratios of AISI 4140, AISI 4340 and AISI 5140 steels in 3.5 *w*/% NaCl environment

		4140			5140			4340		
		f (Hz)		ξ (%)	*f* (Hz)		ξ (%)	*f* (Hz)		ξ (%)
	Mod	FEM	MA		FEM	MA		FEM	MA	
Ref	1	2550,6	2677,24	2,087	2550,4	2670,09	1,922	2550,6	2653,45	1,019
	2	6646,9	6818,45	0,118	6645,3	6911,22	0,022	6646,9	6886,83	0,011
1	1	2550,2	2676,21	2,139	2550,1	2669,62	1,927	2550,4	2652,8	1,040
	2	6645,9	6818,03	0,192	6644,5	6910,91	0,023	6646,5	6886,49	0,025
7	1	2550,1	2674,54	2,158	2550	2669,07	1,928	2550,3	2652,12	1,045
	2	6645,7	6817,92	0,223	6644,4	6910,26	0,023	6646,2	6886,21	0,025
15	1	2550,1	2673,74	2,161	2550	2668,44	1,932	2550,1	2651,6	1,053
	2	6645,7	6816,23	0,234	6644,4	6909,85	0,034	6645,8	6885,97	0,028
30	1	2550	2672,6	2,179	2549,9	2668,16	1,938	2550	2650,87	1,054
	2	6645,5	6815,29	0,240	6644,1	6909,43	0,041	6645,4	6885,78	0,031

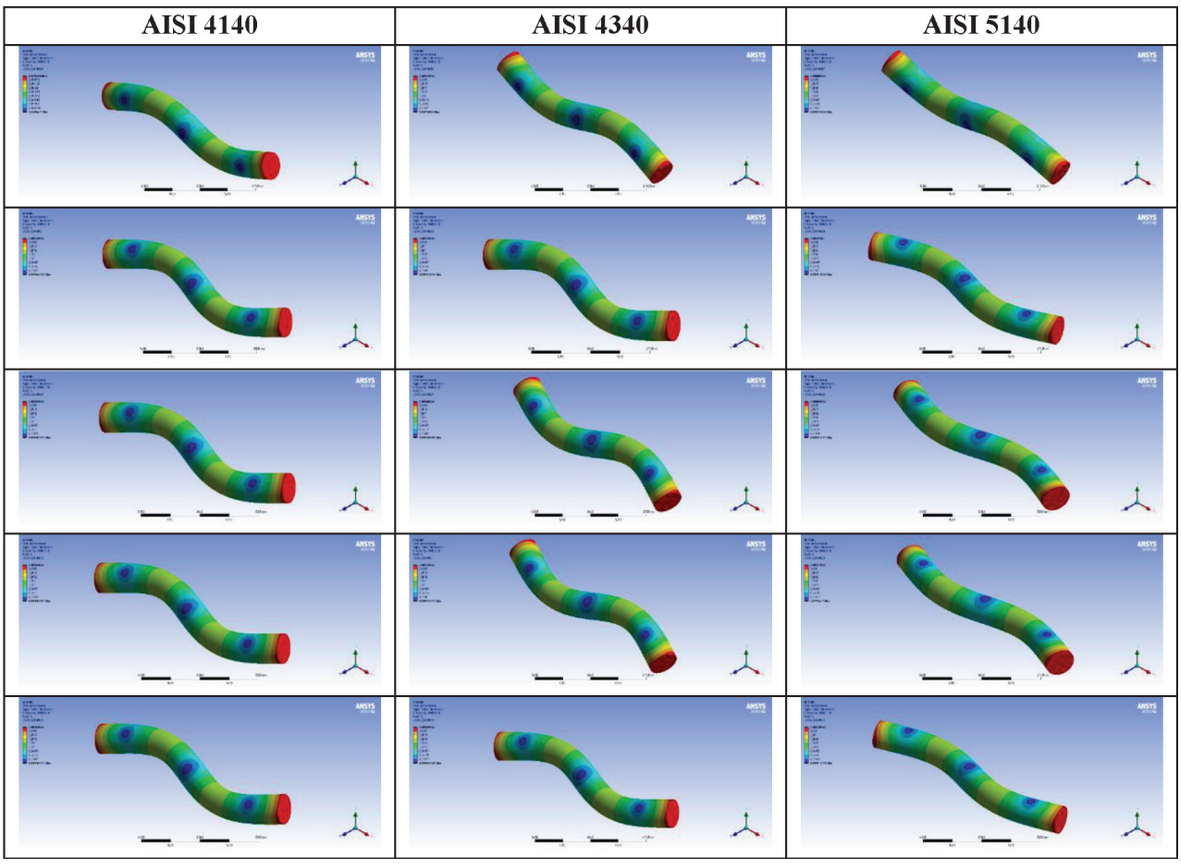

Figure 6: Second natural bending mode shapes of AISI 4140, AISI 4340 and AISI 5140 steels: a) before corrosion, b) 1 d, c) 7 d, d) 15 d, e) 30 d

If the system is undamaged, the excitation force provides free energy to the system, which is used only for the vibrating of the system. In a damaged system, however, some of the free energy will be trapped and dissipated by defects, resulting in less free energy being available for the vibrational motion of the system. The undamaged material takes longer to damp the vibration than the damaged material when the excitation force is stopped and the system is released to damp the vibration. As the level or severity of corrosion increases, the damping ratios obtained generally increase.[35] Therefore, as demonstrated in **Table 5**, the modal analysis showed that the damping ratios of the materials increased with the corrosion time. The mode shapes obtained with FEM for AISI 4140, AISI 4340, and AISI 5140 steel specimens before and after corrosion exposure are displayed in **Figure 5** and **6**. In both frequency modes the bending modes were obtained for AISI 4140, AISI 4340 and AISI 5140 steels. Due to the corrosion of the three metals, it can be observed that both mode shapes change on day 1. Despite the increase in the corrosion exposure time of AISI 4140 metal, there is no change in the two mode shapes. This suggests that the corrosion did not significantly affect the metal's structural integrity. The shapes of the first bending mode of metals AISI 4340 and AISI 5140 remain unchanged after the 7th day, but a change is observed in the shapes of the second bending mode. This suggests that the second bending mode shapes of these metals are more susceptible to change over time compared to their first bending mode shapes.

4 CONCLUSIONS

In this study, changes in the natural frequencies of three different steels corroded in a 3.5 *w*/% NaCl environment were investigated. The inferences obtained with the analysis are as follows:

1. Based on the results obtained with electrochemical corrosion methods, it was found that the corrosion resistance of the three metals decreased by the 15th day, but increased on the 30th day due to the protection provided by the oxide layer formed on the surface. Based on the EIS and dynamic-EIS results, it can be concluded that 4340 metal has the highest corrosion resistance, while 5140 metal has the lowest resistance.

2. Surface analyses showed that the structure of the oxide layer on the surface changed and the thickness of the oxide layer increased with increasing time of exposure to the 3.5 *w*/% NaCl environment.

3. The results obtained with the FEM and modal analysis indicate that the corrosion of metals leads to a reduction in their natural frequencies. When the modal damping ratios were examined, it was found that the damping ratios increased with the increase in the oxide layer formed on the surface, in parallel with the corrosion exposure time.

4. Corrosion caused changes in the mode shapes of the metals. The mode shape of AISI 4140 metal remained unchanged after day 1, while the mode shapes of AISI 4340 and AISI 5140 metals continued to change.

Acknowledgment

This study was supported by the Scientific and Technological Research Council of Turkey (TUBITAK) under Grant Number 123M915. The authors thank TUBITAK for their support. The authors also thank Prof. Dr. Hamit SARUHAN for his contributions.

5 REFERENCES

[1] P. Sathujoda, A novel corrosion detection method using wavelet transformed mode shapes of a functionally graded rotor-bearing system, Composites Part C: Open Access, 5 (**2021**), 100134, doi:10.1016/j.jcomc.2021.100134

[2] A. Bovsunovsky, E. Shtefan, V. Peshko, Modeling of the circumferential crack growth under torsional vibrations of steam turbine shafting, Theor. Appl. Fract. Mech., 125 (**2023**), 103881, doi:10.1016/j.tafmec.2023.103881

[3] J. Zhong, D. Liu, S. Chi, Z. Tu, S. Zhong, Vision-based fringe projection measurement system for radial vibration monitoring of rotating shafts, Mech. Syst. Signal Process., 181 (**2022**), 109467, doi:10.1016/j.ymssp.2022.109467

[4] A. Ahsan Feroz, Harshit, D. Chawla, R. Kumar, To study and analyze the design of drive shafts for automobiles using composite material through empirical review on literature, Mater. Today Proc., 56 (**2022**), 3820–3822, doi:10.1016/j.matpr.2022.01.309

[5] Z. Su, Z. Zheng, X. Huang, H. Hua, Research on dynamic vibration absorber with negative stiffness for controlling longitudinal vibration of propulsion shafting system, Ocean Eng., 264 (**2022**), 112375, doi:10.1016/j.oceaneng.2022.112375

[6] X. Ma, Y. Song, P. Cao, J. Li, Z. Zhang, Self-excited vibration suppression of a spline-shafting system using a nonlinear energy sink, Int. J. Mech. Sci., 245 (**2023**), 108105, doi:10.1016/j.ijmecsci.2023.108105

[7] G. R. Gillich, Z. I. Praisach, V. Iancu, H. Furdui, I. Negru, Natural Frequency Changes due to Severe Corrosion in Metallic Structures, Strojni'ki vestnik – Journal of Mechanical Engineering, 61 (**2015**) 721–730, doi:10.5545/sv-jme.2015.2674

[8] M. Haghshenas, W. Savich, A Case Study on Fatigue Failure of a Transmission Gearbox Input Shaft, J. Fail. Anal. Prev., 17 (**2017**) 1119–1125, doi:10.1007/s11668-017-0352-x

[9] N. Hou, N. Ding, S. Qu, W. Guo, L. Liu, N. Xu, L. Tian, H. Xu, X. Chen, F. Zaïri, C.L. Wu, Failure modes, mechanisms and causes of shafts in mechanical equipment, Eng. Fail. Anal., 136 (**2022**), 106216, doi:10.1016/j.engfailanal.2022.106216

[10] M. Aryayi, M. R. Hadavi, S. Nickabadi, R. Ansari, Changes of Natural Frequencies of Shafts Due to Pitting Corrosion, J. Fail. Anal. Prev., 22 (**2022**), 1144–1150, doi:10.1007/s11668-022-01403-y

[11] S. X. Li, R. Akid, Corrosion fatigue life prediction of a steel shaft material in seawater, Eng. Fail. Anal., 34 (**2013**), 324–334, doi:10.1016/j.engfailanal.2013.08.004

[12] D. P. Singh, R. P. Verma, P. Singh, Failure analysis of premature failed rear axle shaft of a three wheeler vehicle, Mater. Today Proc., 46 (**2021**), 10372–10375, doi:10.1016/j.matpr.2020.12.540

[13] L. Zhang, L. Sun, L. Dong, Experimental Study on the Relationship between the Natural Frequency and the Corrosion in Reinforced Concrete Beams, Adv. Mater. Sci. Eng., 2021 (**2021**), 1–10, doi:10.1155/2021/9976738

[14] P. Goswami, R. Nandan Rai, A systematic review on failure modes and proposed methodology to artificially seed faults for promoting PHM studies in laboratory environment for an industrial gearbox, Eng. Fail. Anal., 146 (**2023**), 107076, doi:10.1016/j.engfailanal.2023.107076

[15] S. Ramakrishna, J. Sathish, V. D. Raj Kumar, S. Raghu Vamsi, Experimental Investigation on Crack Localization in Steel and Composite Structures by Intersection of First Three Normalized Mode Shape Curves, J. Fail. Anal. Prev., 22 (**2022**), 1970–1981, doi:10.1007/s11668-022-01486-7

[16] Y. B. Bozkurt, H. Kovaci, A. F. Yetim, A. Çelik, Tribocorrosion properties and mechanism of a shot peened AISI 4140 low-alloy steel, Surf. Coat. Technol., 440 (**2022**), 128444, doi:10.1016/j.surfcoat.2022.128444

[17] S. S. Deshpande, P. P. Deshpande, M. J. Rathod, Effect of gas nitrocarburizing post oxidation on electrochemical behaviour of AISI 4140 steel in neutral medium, Mater. Today Proc., 50 (**2022**), 1979–1982, doi:10.1016/j.matpr.2021.09.332

[18] M. R. Danelon, L. S. de Almeida, M. D. Manfrinato, L. S. Rossino, Study of the influence of a gradient gas flow as an alternative to improve the adhesion of Diamond-Like Carbon film in the wear and corrosion resistance on the nitrided AISI 4340 steel, Surf. Interfaces, 36 (**2023**), 102352, doi:10.1016/j.surfin.2022.102352

[19] V. Sabelkin, H. Misak, S. Mall, Fatigue behavior of Zn–Ni and Cd coated AISI 4340 steel with scribed damage in saltwater environment, Int. J. Fatigue, 90 (**2016**), 158–165, doi:10.1016/j.ijfatigue.2016.04.027

[20] J. Jiang, J. Hu, X. Yang, N. Guo, H. Xu, H. Li, Y. Jin, H. Yu, Microstructure and annealing behavior of Cr-coatings deposited by double glow plasma on AISI 5140 steel, Results Phys., 15 (**2019**), 102674, doi:10.1016/j.rinp.2019.102674

[21] E. Wang, H. Yang, L. Wang, The thicker compound layer formed by different NH3-N2 mixtures for plasma nitriding AISI 5140 steel, J. Alloys Compd., 725 (**2017**), 1320–1323, doi:10.1016/j.jallcom.2017.07.281

[22] M. Rizvi, H. Gerengi, S. Kaya, I. Uygur, M. Yildiz, I. Sarioglu, Z. Cingiz, M. Mielniczek, B. El Ibrahimi, Sodium nitrite as a corrosion inhibitor of copper in simulated cooling water, Sci. Rep., 11 (**2021**) 8353, doi:10.1038/s41598-021-87858-9

[23] H. Gerengi, P. Slepski, G. Bereket, Dynamic electrochemical impedance spectroscopy and polarization studies to evaluate the inhibition effect of benzotriazole on copper-manganese-aluminium alloy in artificial seawater, Mater. Corros., 64 (**2013**), 1024–1031, doi:10.1002/maco.201206565

[24] N. H. Vo, T. M. Pham, H. Hao, K. Bi, W. Chen, Experimental and numerical validation of impact mitigation capability of meta-panels, Int. J. Mech. Sci., 231 (**2022**), 107591, doi:10.1016/j.ijmecsci.2022.107591

[25] S. Öztürk, H. Gerengi, M. M. Solomon, G. Gece, A. Yildirim, M. Yildiz, A newly synthesized ionic liquid as an effective corrosion inhibitor for carbon steel in HCl medium: A combined experimental and computational studies, Mater. Today Commun., 29 (**2021**), 102905, doi:10.1016/j.mtcomm.2021.102905

[26] H. Gerengi, I. Uygur, M. M. Solomon, M. Yildiz, H. Goksu, Evaluation of the inhibitive effect of Diospyros kaki (Persimmon) leaves extract on St37 steel corrosion in acid medium, Sustain. Chem. Pharm., 4 (**2016**), 57–66, doi:10.1016/j.scp.2016.10.003

[27] T. Zhang, W. Liu, B. Dong, R. Mao, Y. Sun, L. Chen, Corrosion of Cu-doped Ni–Mo low-alloy steel in a severe marine environment, J. Phys. Chem. Solids, 163 (**2022**), 110584, doi:10.1016/j.jpcs.2022.110584

[28] R. E. Melchers, Effect of small compositional changes on marine immersion corrosion of low alloy steels, Corros. Sci., 46 (**2004**), 1669–1691, doi:10.1016/j.corsci.2003.10.004

[29] W. Wu, X. Cheng, H. Hou, B. Liu, X. Li, Insight into the product film formed on Ni-advanced weathering steel in a tropical marine atmosphere, Appl. Surf. Sci., 436 (**2018**), 80–89, doi:10.1016/j.apsusc.2017.12.018

[30] H. Gerengi, The Use of Dynamic Electrochemical Impedance Spectroscopy in Corrosion Inhibitor Studies, Prot. Met. Phys. Chem., 54 (**2018**), 536–540, doi:10.1134/S2070205118030267

[31] E. S. Sherif, A Comparative Study on the Electrochemical Corrosion Behavior of Iron and X-65 Steel in 4.0 wt % Sodium Chloride Solution after Different Exposure Intervals, Molecules, 19 (**2014**), 9962–9974, doi:10.3390/molecules19079962

[32] E. S. M. Sherif, R. M. Erasmus, J. D. Comins, In situ Raman spectroscopy and electrochemical techniques for studying corrosion and corrosion inhibition of iron in sodium chloride solutions, Electrochim. Acta, 55 (**2010**), 3657–3663, doi:10.1016/j.electacta.2010.01.117

[33] T. Datta, A. D. Pathak, S. Basak, S. Gollapudi, K. K. Sahu, Fractal behavior of surface oxide crack patterns on AISI 4140 high-strength low-alloy steel exposed to the simulated offshore environment, Appl. Surf. Sci. Adv., 5 (**2021**), 100110, doi:10.1016/j.apsadv.2021.100110

[34] Y. Ma, Y. Li, F. Wang, Corrosion of low carbon steel in atmospheric environments of different chloride content, Corros. Sci., 51 (**2009**), 997–1006, doi:10.1016/j.corsci.2009.02.009

[35] H. A. Razak, F. C. Choi, The effect of corrosion on the natural frequency and modal damping of reinforced concrete beams, Eng. Struct., 23 (**2001**), 1126–1133, doi:10.1016/S0141-0296(01)00005-0